Joule

 CellPress

Perspective

Identifying soft breakdown in all-solid-state lithium battery

Changhong Wang,[1,2,3] Tao Deng,[2] Xiulin Fan,[4] Matthew Zheng,[1] Ruizhi Yu,[1] Qingwen Lu,[1] Hui Duan,[1] Huan Huang,[3] Chunsheng Wang,[2,*] and Xueliang Sun[1,*]

SUMMARY

Recent years have witnessed significant advances in all-solid-state lithium batteries (ASSLBs). However, soft breakdown hidden in ASSLBs has been overlooked in most previous research. Moreover, existing assessment criteria are insensitive to detecting soft breakdown. Here, we first discuss the current status of ASSLBs and highlight the challenges of evaluating the soft breakdown phenomenon with the existing evaluation method. A simple but effective strategy—cyclic voltammetry—is then proposed to diagnose soft breakdown in all-solid-state symmetric cells. To establish a standard testing protocol, several critical parameters that have not been well emphasized thus far, including areal capacity, thickness, and porosity of solid electrolytes, are numerically analyzed to understand their significant effect on the energy density of practical all-solid-state pouch cells. With these understandings, we establish a definitive testing benchmark with the aim of guiding the research efforts toward in-depth scientific understanding and practical engineering design.

INTRODUCTION

All-solid-state lithium batteries (ASSLBs) have recently received substantial attention because of their unprecedented safety and high theoretical energy density.[1] To enable ASSLBs, various solid-state electrolytes (SSEs) have been reported, such as sulfides,[2,3] oxides,[4] halides,[5,6] borohydrides,[7] and polymer electrolytes.[8,9] Some of them have demonstrated high ionic conductivity at room temperature, which is even higher than that of liquid electrolytes.[3] However, directly incorporating these SSEs into lithium-ion batteries sacrifices their energy density because inorganic SSEs generally have a higher density than liquid electrolytes. To secure a high energy density, a lithium metal anode is required in solid-state batteries because of its high theoretical capacity (3,860 mAh g^{-1}) and lowest electrochemical potential of all anode materials (−3.040 V versus the standard hydrogen electrode). However, lithium metal has been plagued by lithium dendrite growth.[10] This long-standing challenge may be overcome by inorganic SSEs because of their high elastic modulus.[11–13] To investigate Li metal stability against SSEs, a solid-state symmetric cell with a sandwiched configuration of Li/SSE/Li has been frequently used because of its simplicity. Based on Li/SSE/Li symmetrical results, various advanced strategies have been claimed to be effective in suppressing lithium dendrite growth in SSEs and interfacial reactions.[14–19] At first glance, these advances are very encouraging for the commercialization of ASSLBs. However, there are two misconceptions about Li/SSE/Li symmetric cell research. First, most previous strategies were evaluated with unrealistic assessment metrics such as limited areal capacity, making them

Context & scale

To develop next-generation energy storage systems with high energy density and unprecedented safety, all-solid-state lithium batteries (ASSLBs) that replace conventional flammable organic liquid electrolytes with solid-state electrolytes (SSEs) have been revived in academia and industry. However, soft breakdown hidden in ASSLBs has not been well realized, which generally leads to unreliable conclusions and significantly retards ASSLB development. To exclude this phenomenon, we propose a simple but effective method—cyclic voltammetry—to diagnose the soft breakdown in ASSLBs. Moreover, a low-frequency electrochemical impedance analysis is employed to quantify the soft breakdown phenomenon. Finally, a standard testing protocol is suggested, which could help this community obtain reliable and comparable results in the future. This work's fundamental understanding and established assessment metrics are also applicable to other metal-based all-solid-state batteries.

Joule
Perspective

impractical to incorporate into practical all-solid-state pouch cells. Second, some Li/SSE/Li symmetric cells demonstrated deceptive cycling stability because of the unawareness of soft breakdown.[20,21]

What is a soft breakdown phenomenon? Ideally, the charge carrier of a solid-state symmetric cell should be only ions. If a Li/SSE/Li symmetric cell has both ion and electron transport, it is a soft breakdown (Figure 1A). If a cell has only electron transport, that is called hard breakdown. To the best of our knowledge, the soft breakdown phenomenon is very common in solid-state batteries but has been overlooked until now, most likely due to the lack of an effective method to identify it. Therefore, it is necessary and urgent to propose a simple but effective method to identify the soft breakdown phenomenon and then establish a testing benchmark for the research community of ASSLBs so that all future endeavors can be unanimously used for the practical application of ASSLBs.

To this end, we first review the current status of solid-state Li/SSE/Li symmetric cells and then highlight some unrealistic assessment criteria in the literature, which is perhaps related to the unawareness of soft breakdown in ASSLBs. Then, a simple but effective diagnosis method—cyclic voltammetry (CV)—is proposed to identify the soft breakdown. Furthermore, the degree of soft breakdown can be quantitively determined by low-frequency electrochemical impedance spectroscopy (EIS) analysis. In order to establish a standard protocol for Li/SSE/Li symmetric cell investigation, several overlooked technical parameters, including the areal capacity of Li metal, SSE thickness, and porosity, are numerically evaluated to reveal their effect on the gravimetric and volumetric energy density of practical all-solid-state pouch cells. With these in-depth understandings, a standard testing protocol for Li/SSE/Li symmetric cells is finally established and recommended, which should be implemented in future research to help obtain reliable and comparable results for both scientific understanding and practical engineering design. We hope this work can draw attention to the fact that strict evaluation of lithium metal anode should base on practical energy density targets so that new advances and strategies can effectively incorporate into practical high-energy-density ASSLBs.

RESULTS

Status of solid-state Li/SSE/Li symmetric cells and corresponding ASSLBs

We first reviewed the current status of solid-state symmetric cells (Li/SSE/Li) and their corresponding ASSLBs. Several abnormal phenomena merit special attention here. (1) Many Li/SSE/Li symmetric cells demonstrated long-term stability but a minimal areal capacity (0.01–0.5 mAh.cm^{-2}) (Figure 1B).[22–32] Such a limited areal capacity corresponds to only 50 nm–2.5 μm of Li plated and stripped. Considering that a thick Li (~460 μm) was normally used in those reports, the fraction of Li metal that was platted and stripped is only 0.01%–0.5%, which means the volume change of Li metal anode in ASSLBs was not revealed in those reports. (2) The plated capacity of symmetric cells is sometimes lower than their corresponding all-solid-state full cells. This discrepancy raises the question of why a Li/SSE/Li symmetric cell is only plated/stripped with a shallow capacity (e.g., 0.1 mAh.cm^{-2}) if a lithium metal anode can be cycled with a large areal capacity (e.g., 1 mAh.cm^{-2}) in all-solid-state full cells (Figure 1B). (3) Some references demonstrated Li metal stability against Li metal with very limited areal capacity but large current density, i.e., a small areal capacity of 0.25 mAh.cm^{-2} with a high current density of 8.6 mA.cm^{-2},[33] 0.004167 mAh.cm^{-2} cycled by 0.05 mA.cm^{-2}.[34] In these cases, the Li/SSE/Li symmetric cells were only

[1]Department of Mechanical and Materials Engineering, University of Western Ontario, 1151 Richmond St., London, ON N6A 3K7, Canada

[2]Department of Chemical and Biomolecular Engineering, University of Maryland, College Park, MD 20740, USA

[3]Glabat Solid-State Battery Inc., London, ON N6G 4X8, Canada

[4]State Key Laboratory of Silicon Materials, School of Materials Science and Engineering, Zhejiang University, Hangzhou 310027, China

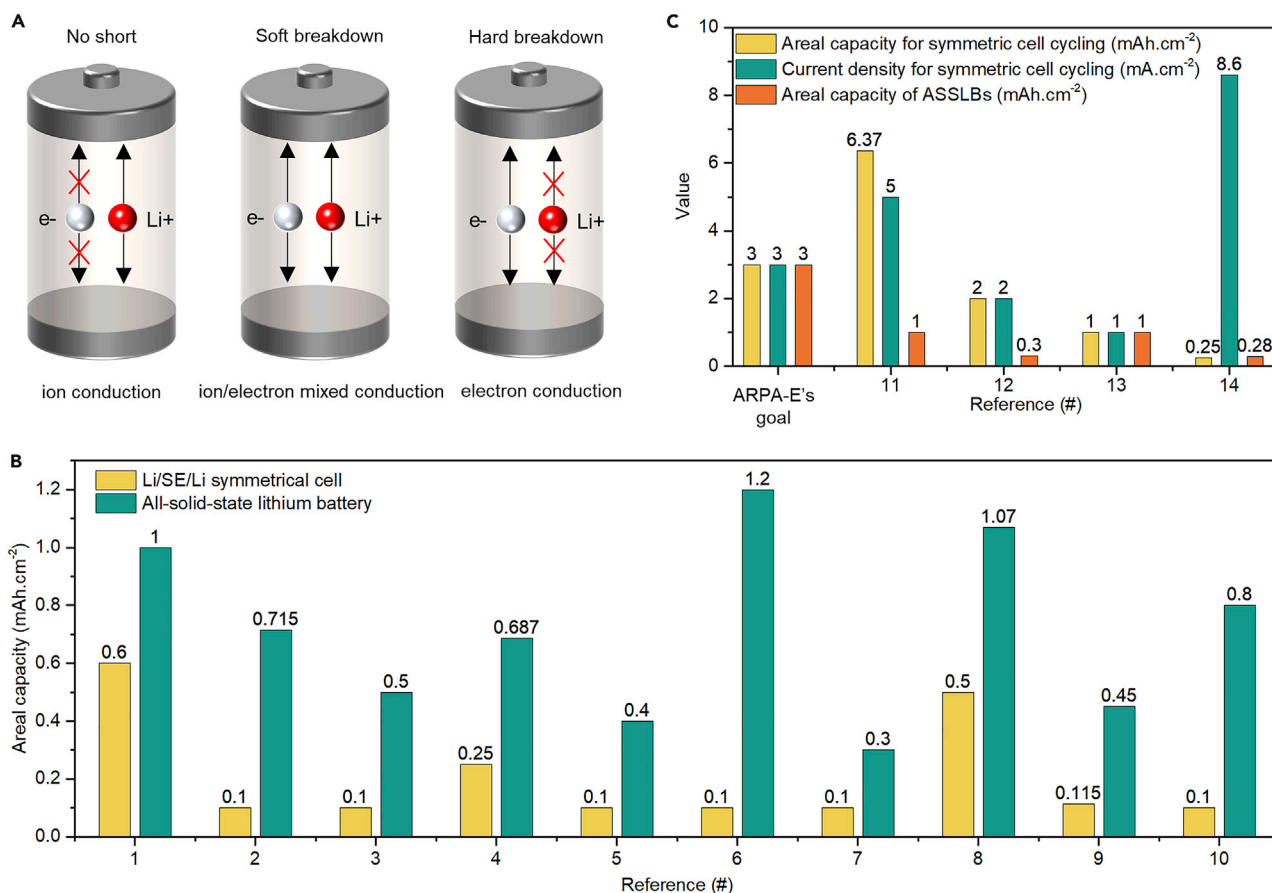*Correspondence: cswang@umd.edu (C.W.), xsun9@uwo.ca (X.S.)

https://doi.org/10.1016/j.joule.2022.05.020

Joule
Perspective

🕭 CellPress

Figure 1. Status of Li/SSE/Li symmetric cells and their corresponding ASSLBs
(A) Schematical diagram of all-solid-state batteries with different conduction mechanisms.
(B) The disparity of cycling capacity between Li/SSE/Li symmetric cells and corresponding ASSLBs.
(C) High-performance all-solid-state lithium symmetric cells. The reference data were summarized in Table S1.

charged/discharged in just a few minutes, indicating that interfacial reactions are minimized due to their very short plating/stripping time.[35] (4) It is encouraging that several references have demonstrated high areal capacities (i.e., 1, 2, and 5 mAh cm^{-2}) with good cycling stability (Figure 1C).[36–38] However, these reports did not verify whether the symmetric cells have a soft breakdown or not, which may be due to the unawareness of the soft breakdown phenomenon in Li/SSE/Li and the lack of an effective method to identify it.

These abnormal phenomena have significantly retarded the progress of improving Li metal anodes for practical engineering of ASSLBs, mainly due to arbitrary testing parameters and ignorance of soft breakdown. In fact, soft breakdown phenomena in solid-state symmetric cells are pretty common because of the high electronic conductivity of SSE, poor interfacial solid-solid ionic contact, and uneven localized electric field.[39,40] As shown in Figures S1–S3, the soft breakdown is observed in all-solid-state Li symmetric cells with various SSEs, including oxide electrolytes (i.e., $Li_{6.5}La_3Zr_{1.5}Ta_{0.5}O_{12}$ [LLZTO]), halide electrolytes (i.e., Li_3ScCl_6), and sulfide electrolytes (e.g., $Li_{10}GeP_2S_{12}$ [LGPS]). The soft breakdown phenomenon leads to deceptive lithium stability, which is challenging to identify just by looking into plating and stripping curves and/or simple EIS analysis.
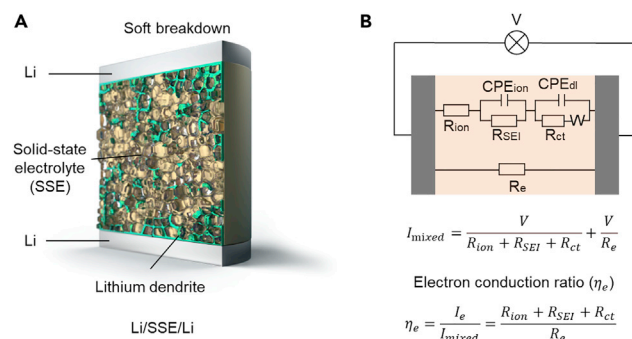
Figure 2. Qualitative and quantitative analysis of soft breakdown by CV
(A) Illustration of lithium dendrite formation in Li/SE/Li symmetric cells with a soft breakdown.
(B) An equivalent circuit describes the ion and electron transport inside the symmetric cell after the soft breakdown.

Under this circumstance, we propose that CV could be used to identify the soft breakdown. In principle, the electrochemical process of Li plating and stripping will be identified by CV if the symmetrical cell has no electron transport. In contrast, CV will show a linear response if the symmetrical cell has a hard breakdown, which indicates no interfacial electrochemical process occurs. For a Li/SSE/Li symmetric cell with soft breakdown, CV will show a mixed state of both electrochemical process and electronic conduction. Therefore, CV is a simple but effective method to diagnose the soft breakdown phenomenon in solid-state symmetric cells.

Proposing cyclic voltammetry to identify the soft breakdown of solid-state symmetric cells

Figure 2A schematically illustrates a cross-sectional image of a Li/SSE/Li symmetric cell with a soft breakdown, in which lithium dendrites grow at the grain boundaries but are not connected.[39,40] In this case, an equivalent circuit can be built to simulate the symmetric cell, as shown in Figure 2B. Ion transport is governed by the resistance of SSEs and interfacial resistance between Li metal and SSEs. The interfacial resistance includes charge transfer resistance (R_{ct}) and resistance of the interphase (R_{SEI}).[41] Electron transport is limited by the electrical resistance of SSEs. Therefore, the overall current combines electronic current and ionic current in the symmetric cell, as expressed by Equation 1 below.

$$I_{mixed} = I_{ion} + I_e = \frac{V}{R_{ion} + R_{SEI} + R_{ct}} + \frac{V}{R_e} \qquad \text{(Equation 1)}$$

where I_{mixed} represents the peak current of solid-state symmetric cells in CV. I_{ion} is the ionic current contributed by ion transport, whereas I_e is the electronic current from electron transport. V is the applied bias on the solid-state symmetric cells. R_{ion} is the resistance of SSEs. R_{SEI} represents the resistance of the interphase between SSEs and Li metal, R_{ct} represents charge transfer resistance, and R_e is the electric resistance of SSEs, which describes the electron transport in the symmetric cell.

If there are no interfacial reactions and degradation of SSEs, the CV current should remain the same upon cycling, as demonstrated by the symmetric cells with liquid electrolytes.[42] If there are some interfacial reactions and/or SSE degradation, the current should become smaller and smaller due to the increase of R_{ion} and R_{int}. Only R_e becomes smaller, we can observe the current increases in the CV profile. Therefore, the soft and hard breakdowns of Li/SSE/Li symmetric cells can be identified by just determining the current change of the CV profile.

To quantify the electron transport portion in Li/SSE/Li cells with soft breakdown, we can use low-frequency EIS to determine the electronic resistance of SSEs after the soft breakdown. The electronic current ratio (η_e) caused by the soft breakdown can be quantified as below.

$$\eta_e = \frac{I_e}{I_{mixed}} \times 100\% = \frac{R_{ion} + R_{SEI} + R_{ct}}{R_e} \times 100\% \qquad \text{(Equation 2)}$$

Before cycling, R_e is hundreds and thousands of times higher than R_{ion} and R_{int}. Therefore, η_e is close to zero, implying no electron transport at all. The ionic current mainly contributes the overall current. As the lithium dendrite grows, R_e becomes smaller because lithium dendrite forms inside SSEs, which is inductive to electron tunneling; thus, the electronic current increases. As a result, η_e becomes larger and larger. In addition, the electronic current increase ratio ω can be expressed by Equation 3:

$$\omega = \frac{\Delta I}{I_{initial}} = \frac{I_{after} - I_{initial}}{I_{initial}} \times 100\% \qquad \text{(Equation 3)}$$

In light of this theoretical understanding, CV can be used to qualitatively detect the soft breakdown of a solid-state Li/SSE/Li symmetric cell after long-term cycling. In addition, low-frequency EIS analysis can be employed to quantitively determine the degree of soft breakdown in the solid-state symmetric cells.

Qualitative and quantitative analyses of soft breakdown by cyclic voltammetry and EIS

To prove the effectiveness of the above-mentioned electrochemical analyses, we performed CV analysis on the Li/LGPS/Li and Li/Li$_6$PS$_5$Cl/Li symmetric cells after long-term cycling. Li/LGPS/Li symmetric cells were platted and stripped with a current density of 3 mA.cm^{-2} and an areal capacity of 3 mAh.cm^{-2} (Figure 3A). Surprisingly, Li/LGPS/Li symmetric cells can be cycled under this practical condition but show an extremely large overpotential. The voltage drops slowly after 25 h and stabilizes at 0.8 V after 100 h, which indicates the typical soft breakdown phenomenon, not an interface stabilization process.[43,44] Before the soft breakdown, the peak current of Li/LGPS/Li is gradually reduced due to the degradation of LGPS (Figure 3B). In contrast, the CV peak current of the Li/LGPS/Li after a soft breakdown is gradually increased (Figure 3C), which is indicative of substantial electron transport inside Li/LGPS/Li. The reason for this soft breakdown is that LGPS will ultimately turn into a mixed electron/ion conductor due to the formation of Li$_x$Ge alloys, Li$_3$P, and Li$_2$S interphase, which is ion/electron conductive.[45] Therefore, we can see a "deceptive Li stability" over a long time. Another supplementary method to identify the soft breakdown of Li/SSE/Li is to determine the leakage current after cycling. If the leak current significantly increases, which is also indicative of electron transport. The leakage current of Li/LGPS/Li symmetric cells is three times higher after soft breakdown (Figure S4).

Not only does Li$_{10}$GeP$_2$S$_{12}$ show the soft breakdown phenomenon but so does Li$_6$PS$_5$Cl. Unlike Li$_{10}$GeP$_2$S$_{12}$, Li$_6$PS$_5$Cl is free of metal ions. Therefore, Li$_6$PS$_5$Cl forms ion-conducting interphase at the interface.[46,47] As the Li/Li$_6$P$_5$SCl/Li symmetrical cell cannot be cycled under 3 mAh.cm^{-2} (Figure S5) because of hard breakdown, as identified when we tested it at 0.2 mA.cm^{-2} with 0.2 mAh.cm^{-2}. This symmetric cell shows a "soft breakdown" after 20 h and a hard breakdown after 230 h (Figure 3D). The CV profile of the Li/Li$_6$P$_5$SCl/Li shows that after the first cycle, the peak current suddenly increases and then stabilizes (Figure 3E), which also hints
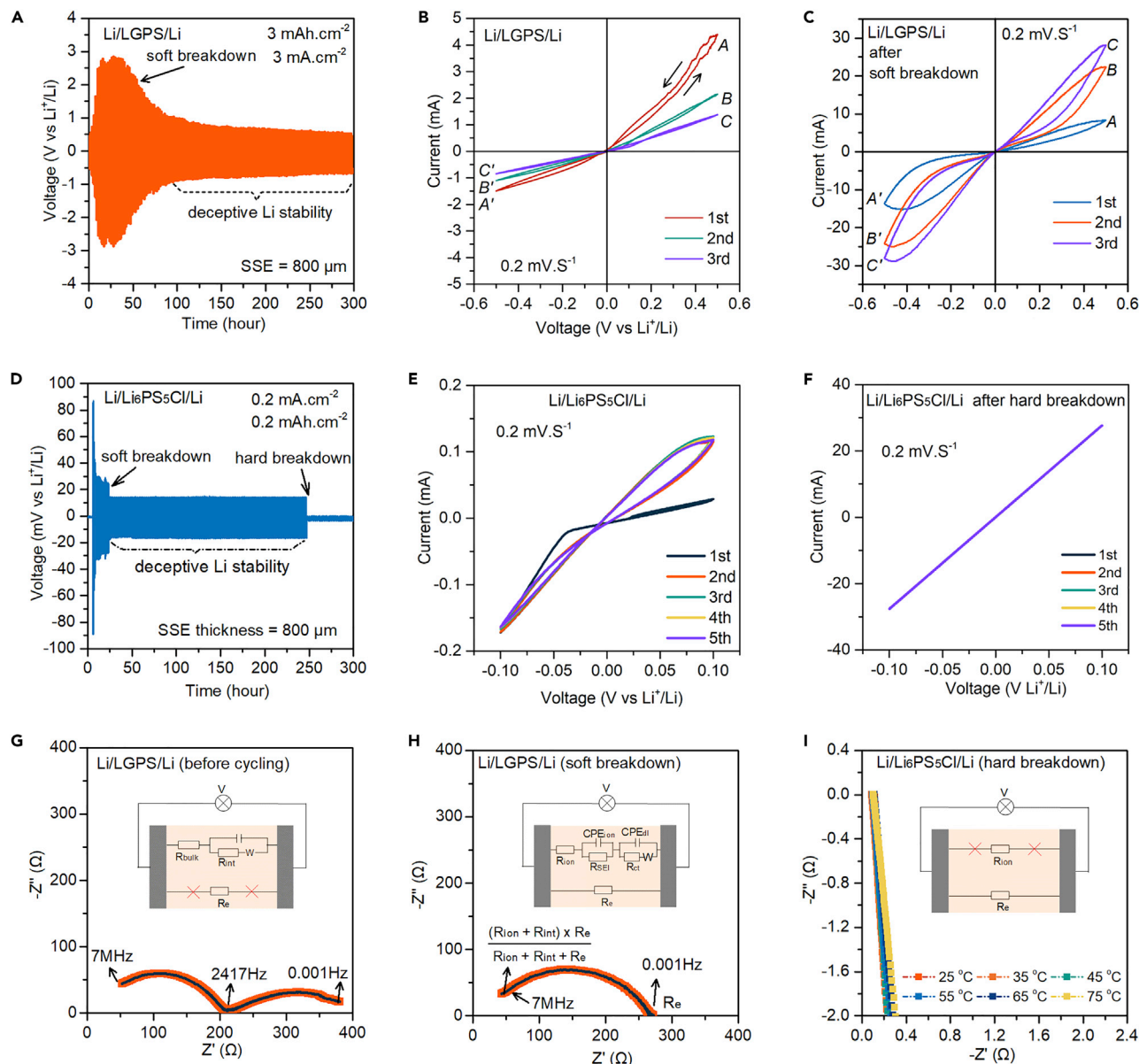
Figure 3. Qualitative and quantitative analyses of soft breakdown by cyclic voltammetry and EIS

(A) Li$^+$ plating/stripping behavior in Li/LGPS/Li symmetric cells under the condition of 3 mA cm^{-2} and 3 mAh cm^{-2}.

(B) CV profiles of pristine Li/Li$_{10}$GeP$_2$S$_{12}$/Li symmetric cells.

(C) CV profiles of Li/LGPS/Li symmetric cells with soft breakdown.

(D) Li$^+$ plating/stripping behavior in Li/Li$_6$PS$_5$Cl/Li symmetric cells under the condition of 0.2 mA cm^{-2} and 0.2 mAh cm^{-2}.

(E) CV profiles of pristine Li/Li$_6$PS$_5$Cl/Li symmetric cells.

(F) CV profiles of Li/Li$_6$PS$_5$Cl/Li symmetric cells with hard breakdown.

(G) EIS spectra of Li/LGPS/Li symmetric cells before cycling.

(H) EIS spectra of Li/LGPS/Li symmetric cells with soft breakdown.

(I) Temperature-dependent EIS profiles of Li/Li$_6$PS$_5$Cl/Li symmetric cells with hard breakdown.

at both ion and electron transport. Therefore, deceptive lithium stability is well observed. After the hard breakdown, the CV profile only shows a linear line, which equals a resistor (Figure 3F). These experimental analyses demonstrated that CV is a simple but straightforward method to diagnose the soft breakdown phenomenon in solid-state symmetric cells.

Low-frequency EIS was further employed to quantify the electron transport contribution to the overall leakage current. Taking Li/LGPS/Li as an example, the EIS profile of Li/LGPS/Li before cycling shows a semicircle at the high and middle frequencies and a depressed semicircle, which can be ascribed to the interfacial resistance between Li and SSE (R_{int}), which consists of the resistance of an interphase (R_{SEI}) and charge transfer resistance (R_{ct}) (Figure 3G).[41] After the soft breakdown, the intersection of the high frequency (7 MHz) line with the real axis is the resistance of the electronic and ionic resistance in parallel, and the intersection of the low-frequency (0.001 Hz) line with the real axis is the electronic resistance (R_e) (Figure 3H).[48] Based on this understanding, the electronic conductivity of Li/LGPS/Li after soft breakdown can be quantified (4.782×10^{-4} S.cm^{-1}), which is five orders of magnitude higher than pristine LGPS (10^{-9} S.cm^{-1}). After the hard breakdown (Li/Li$_6$PS$_5$Cl/Li), the EIS only shows an inductive line (Figure 3H), which means a strong lithium dendrite contacting both electrodes and resulting in a hard breakdown. With rational low-frequency EIS analysis, the electronic conductivity of Li/SSE/Li after soft breakdown can be quantified.

Alternative methods to detect soft breakdown

It should be mentioned that the soft breakdown phenomenon is common to all metal batteries, particularly under high current densities and large capacities, but it is challenging to be detected no matter in liquid or solid-state systems.[49,50] For instance, C. Zhi's group pointed out the soft breakdown phenomenon of aqueous Zn-ion batteries and proposed several alternative methods to detect soft breakdown,[51] including (1) determining activation energy using low-temperature EIS analysis,[10] (2) interfacial charge transfer resistance analysis,[51] (3) validating the overpotential after tuning the current density (an unchanged or lower overpotential under higher current density is an indicator of soft breakdown), and (4) using asymmetrical cells (with thin metal anodes) or full cells, in which the fluctuation of charge curves (or upper cut-off voltage cannot be reached) is a good indicator of soft breakdown.[52–54] We also attempted to determine the activation energy of Li/SSE/Li solid-state symmetric cells after soft breakdown. The activation energy is reduced after soft breakdown for relatively stable SSEs, e.g., Li$_6$PS$_5$Cl (Figure S6). For Li-unstable SSEs such as LGPS, activation energy cannot be determined via temperature-dependent EIS analysis (Figure S7) because of the side reactions between lithium dendrites and LGPS. Therefore, using low-temperature EIS analysis is more accurate in obtaining the activation energy, which can minimize the side reactions.[51] Furthermore, full cell (or asymmetrical cell) analysis is the most direct way to identify the soft breakdown. The fluctuation of charge curves and the over-charge phenomenon of the all-solid-state full cell are related to the soft breakdown of SSEs (Figure S8), which lead to the low Coulombic efficiency. Therefore, we advocate a comprehensive analysis of all-solid-state batteries to exclude soft breakdown, which is pivotal for practical advances in all-solid-state battery technology.

Key parameters determining attainable energy density of all-solid-state lithium batteries

Before establishing a standard testing protocol, we need to understand which parameters are essential and how they affect the energy density of practical all-solid-state pouch cells. Here, we would like to emphasize that the most important parameter for evaluating Li/SSE/Li symmetric cells is the areal capacity of Li metal cycled. Based on high areal capacity, other parameters can be fairly evaluated, including cycling life, current density, critical current density, and Coulombic efficiency. Furthermore, the thickness and porosity of SSEs, which generally were unspecified in previous literature, should be clarified in future reports. Based on the industrial
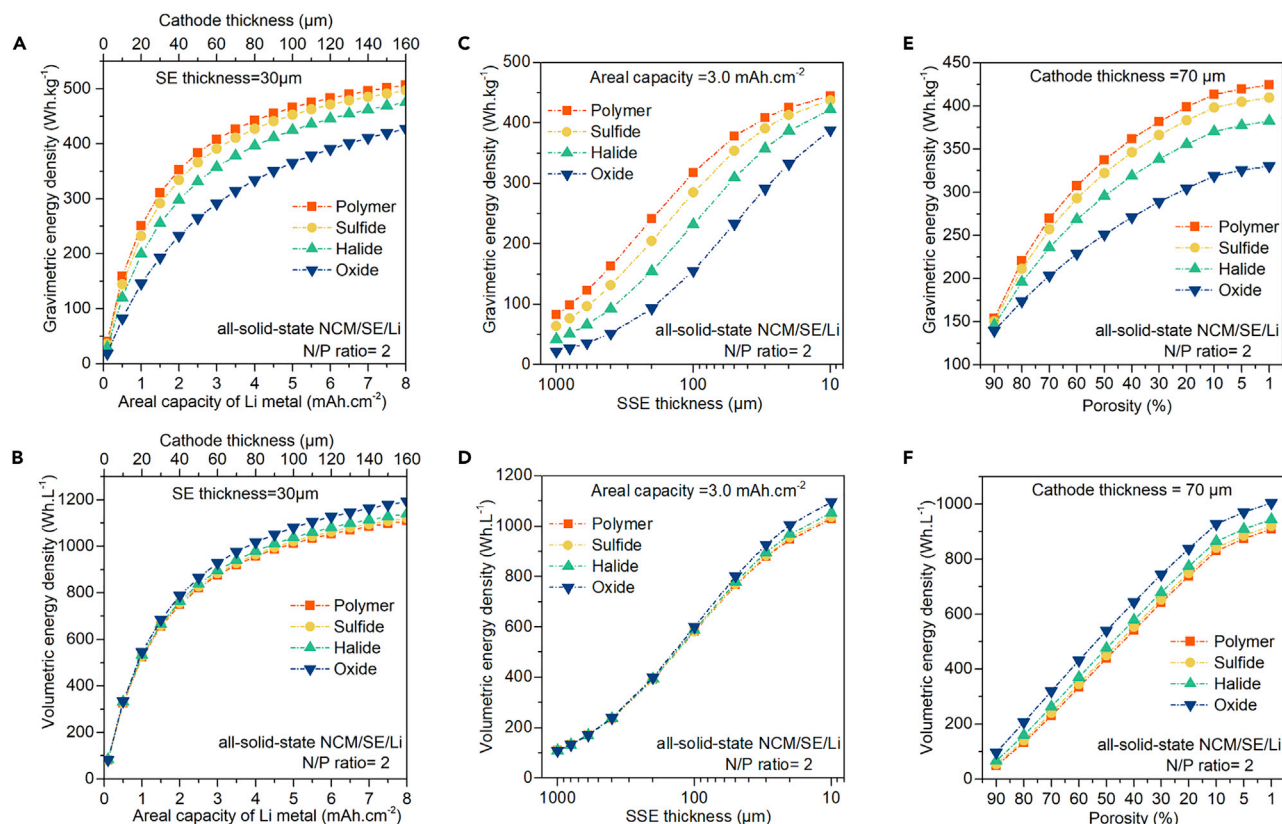
Figure 4. Effect of areal capacity, SE thickness, and porosity on the gravimetric and volumetric energy density of all-solid-state lithium metal batteries

(A) Areal-capacity-dependent gravimetric energy density, (B) areal-capacity-dependent volumetric energy density, (C) SE thickness-dependent gravimetric energy density, (D) SE thickness-dependent volumetric energy density, (E) porosity-dependent gravimetric energy density, and (F) porosity-dependent volumetric energy density.

standard parameters, we numerically analyzed the effect of the areal capacity of Li metal, SSE thickness, and porosity on gravimetric and volumetric energy density.[55,56] (1) If Li metal anodes are cycled with an areal capacity less than 1 mAh cm^{-2}, the gravimetric energy density of ASSLBs will not go beyond 200 Wh.kg^{-1}, no matter what kinds of SSEs are used (Figure 4A). To realize an energy density over 300 Wh.kg^{-1}, the minimum requirement of Li metal capacity is 3 mAh.cm^{-2}. The corresponding volumetric energy density will reach 800 Wh.L^{-1} (Figure 4B). If 4 mAh.cm^{-2} is fully utilized, the attainable energy density is 400 Wh.kg^{-1}. As guided by ARPA-E IONICS, 3 mAh.cm^{-2} can be set as the first target that needs to be realized in Li/SSE/Li symmetric cells without any soft break-down. (2) The SSE thickness also plays a crucial role in attainable energy density.[57,58] As shown in Figure 4C, with 500–1,000 μm thick SSEs, the attainable energy density will not exceed 150 Wh.kg^{-1}. To meet 300 Wh.kg^{-1}, the thickness of SSE should be less than 30 μm. The corresponding volumetric energy density is close to 900 Wh.L^{-1} (Figure 4D). Therefore, continuous research efforts should be devoted to thin SSE fabrication, and a target of 30 μm should be realized.[56,59–62] (3) The porosity of SSEs and composite electrodes should also be considered, which has not been well emphasized yet. The porosity of SSEs also has a significant effect on the lithium dendrite growth and solid-solid ionic contact. Based on our numerical analysis, the porosity of SSEs and composite electrodes should be less than 10% to attain competitive volumetric and gravimetric energy density (Figures 4E and 4F). (4) The

Table 1. Recommend evaluation protocol for Li/Li symmetric cells

Step 1: control electrolyte	the porosity and thickness of SSE should be given. The ideal SSE thickness is 30 μm.
Step 2: thin Li metal	a thin Li metal foil should be used for future research (i.e., 30 μm for 3 mAh.cm^{-2}, 40 μm for 4 mAh.cm^{-2}, keeping the N/P ratio as 2)
Step 3: control capacity to evaluate cycling life	set the areal capacity as 3 mAh.cm^{-2} for the Li plating/stripping cycle. The current density can be 1–3 mA.cm^{-2}.
Step 4: exclude soft breakdown	after long-term cycling, cyclic voltammetry should be analyzed to check if the cell has a soft breakdown or not.
Step 5: test critical current density	set the cycling capacity as 3 mAh.cm^{-2}. Then adjust the current density from C/10 (0.3 mA.cm^{-2}) to 4C (12 mA.cm^{-2}). Run the cell for at least 5–10 cycles under each current density.
15 μm Li/SSE/30 μm Li	
Step 5: Coulombic efficiency testing	set the cycling capacity as 3 mAh.cm^{-2}, count how many cycles 15 μm Li metal can last, and then calculate the average Coulombic efficiency for 15 μm Li. This average Coulombic efficiency can predict the real cycle life of ASSLBs.

pressure of ASSLBs should be standardized for comparison. The volume change can be fairly evaluated with a thin Li metal anode. Using external pressure to improve the battery cycling is required. Therefore, the pressure for battery cycling should also be given. Otherwise, the reported results are hard to be reproduced. This numerical analysis delivers several takeaways: (1) the minimum areal capacity of 3 mAh.cm^{-2} should be guaranteed in the future Li/SSE/Li cells, (2) the thickness and porosity of SSEs should be clarified, (3) thin Li metal (<30 μm) should be used in future research, and (4) the pressure and temperature for testing should also be articulated in future reports.

Establishing a standard testing protocol for Li/SSE/Li symmetrical cells

Based on the insightful discussion above, we propose a standard protocol for evaluating Li/SSE/Li symmetric cells, as listed in Table 1. (1) When making Li/SSE/Li symmetric cells or ASSLBs, the thickness and porosity of SSEs should be given. Preferably, the thickness of SSE should be less than 50 μm. The ideal porosity of SSEs should be less than 10%. We recommend the solvent-free method to fabricate thin and freestanding SSE membranes.[59,60] (2) A thin lithium metal anode should be cycled with a large areal capacity. As suggested by ARPA-E IONIC, it is better to test lithium metal anode with 3 mA.cm^{-2} and 3 mAh.cm^{-2}. This practical testing benchmark can demonstrate how effective the applied strategy is. (3) After long-term cycling, CV and low-frequency EIS should be performed and analyzed to identify and avoid deceptive Li stability. (4) Critical current density also should be tested with a large cycling capacity of 3 mAh cm^{-2}. The maximum current density can be 12 mA.cm^{-2} to simulate fast charging capability. Under each current density, Li/SSE/Li should be cycled at least 5–10 cycles for each current density, not just one cycle as most researchers do. (5) To obtain the Coulombic efficiency, we suggest using asymmetric cells (e.g., 15 μm Li/SSE/30 μm Li), in which the average Coulombic efficiency can be calculated to predict practical battery life.[63] The operating pressure and temperature should be given. Following these rules, we believe the future research could be fairly compared and even incorporated into practical solid-state lithium metal pouch cells.

DISCUSSION

In this perspective, we started with a literature survey of ASSLBs and pointed out the unawareness of soft breakdown and random testing parameters, which have significantly retarded the commercial progress of ASSLBs. Then, a simple but effective method—CV—is proposed to diagnose the soft breakdown hidden in all-solid-state

symmetric cells, which can effectively exclude the deceptive Li metal stability in symmetrical solid-state cells in the future. In combination with rational analysis of low-frequency EIS, the self-discharge of solid-state symmetric cells caused by soft breakdown can be quantitatively determined. In the end, a standard testing protocol for Li/SSE/Li symmetric is established and outlined, allowing all future research to be fairly compared and centralized toward a specific energy density target (i.e., 400 or 500 Wh.kg^{-1}). Using thin Li metal and ultrathin SSEs is necessary for future research, which can help identify the technical engineering issues early. This work's fundamental understanding and established assessment metrics are also applicable to other metal-based solid-state batteries, such as Na-metal batteries.

METHOD

$Li_{10}GeP_2S_{12}$ and Li_6PS_5Cl were supplied by MSE Supplier. The LLZTO powder was purchased from Tai'an City Faraday Energy Technology. Li_3ScCl_6 was synthesized in our lab, as described in our previous paper.[43] To make the solid-state lithium symmetric cells, 100 mg solid electrolytes were uniaxially pressed into a 10 mm pellet under 380 MPa in a homemade mold cell. Then Li foils were attached on both sides of SE pellets and pressed at 50 MPa. The symmetric cells with Li/SSE/Li configuration were assembled in an ultra-pure argon-filled glove box. The Li stripping/plating studies were carried out using NEWARE battery analyzers with a voltage range of 0–5 V and a current range of 10 mA at room temperature. Constant current densities were applied to the electrodes during repeated stripping/plating while the potential was recorded over time. Electrochemical impedance analysis was performed on a biologic electrochemical station with a frequency range from 7 to 1 MHz with an amplitude of 10 mV. CV was also performed on a biologic electrochemical station with a scan rate of 0.2 mV.S^{-1}. The numerical analysis of attainable energy density of practical all-solid-state pouch cells with a dimension of 10 × 5 cm^2 was performed in accordance with Liu et al.[55] and Wang et al.[56]

DATA AVAILABILITY

The datasets analyzed and generated during this study are included in supplemental information.

SUPPLEMENTAL INFORMATION

Supplemental information can be found online at https://doi.org/10.1016/j.joule.2022.05.020.

DECLARATION OF INTERESTS

The authors declare no competing interests.

REFERENCES

1. Xiao, Y., Turcheniuk, K., Narla, A., Song, A.-Y., Ren, X., Magasinski, A., Jain, A., Huang, S., Lee, H., and Yushin, G. (2021). Electrolyte melt infiltration for scalable manufacturing of inorganic all-solid-state lithium-ion batteries. Nat. Mater. 20, 984–990. https://doi.org/10.1038/s41563-021-00943-2.

2. Kato, Y., Hori, S., Saito, T., Suzuki, K., Hirayama, M., Mitsui, A., Yonemura, M., Iba, H., and Kanno, R. (2016). High-power all-solid-state batteries using sulfide superionic conductors.

Joule
Perspective

CellPress

Nat. Energy 1, 16030. https://doi.org/10.1038/nenergy.2016.30.

3. Hayashi, A., Masuzawa, N., Yubuchi, S., Tsuji, F., Hotehama, C., Sakuda, A., and Tatsumisago, M. (2019). A sodium-ion sulfide solid electrolyte with unprecedented conductivity at room temperature. Nat. Commun. 10, 5266. https://doi.org/10.1038/s41467-019-13178-2.

4. Wang, C., Fu, K., Kammampata, S.P., McOwen, D.W., Samson, A.J., Zhang, L., Hitz, G.T., Nolan, A.M., Wachsman, E.D., Mo, Y., et al. (2020). Garnet-type solid-state electrolytes: materials, interfaces, and batteries. Chem. Rev. 120, 4257–4300. https://doi.org/10.1021/acs.chemrev.9b00427.

5. Asano, T., Sakai, A., Ouchi, S., Sakaida, M., Miyazaki, A., and Hasegawa, S. (2018). Solid halide electrolytes with high lithium-ion conductivity for application in 4 V class bulk-type all-solid-state batteries. Adv. Mater. 30, e1803075. https://doi.org/10.1002/adma.201803075.

6. Li, X., Liang, J., Yang, X., Adair, K.R., Wang, C., Zhao, F., and Sun, X. (2020). Progress and perspectives on halide lithium conductors for all-solid-state lithium batteries. Energy Environ. Sci. 13, 1429–1461. https://doi.org/10.1039/C9EE03828K.

7. Maekawa, H., Matsuo, M., Takamura, H., Ando, M., Noda, Y., Karahashi, T., and Orimo, S.-i. (2009). Halide-stabilized LiBH4, a room-temperature lithium fast-ion conductor. J. Am. Chem. Soc. 131, 894–895. https://doi.org/10.1021/ja807392k.

8. Meyer, W.H. (1998). Polymer electrolytes for lithium-ion batteries. Adv. Mater. 10, 439–448. https://doi.org/10.1002/(SICI)1521-4095(199804)10:6<439::AID-ADMA439>3.0.CO;2-I.

9. Zhao, Q., Liu, X., Stalin, S., Khan, K., and Archer, L.A. (2019). Solid-state polymer electrolytes with in-built fast interfacial transport for secondary lithium batteries. Nat. Energy 4, 365–373. https://doi.org/10.1038/s41560-019-0349-7.

10. Albertus, P., Babinec, S., Litzelman, S., and Newman, A. (2018). Status and challenges in enabling the lithium metal electrode for high-energy and low-cost rechargeable batteries. Nat. Energy 3, 16–21.

11. Monroe, C., and Newman, J. (2005). The impact of elastic deformation on deposition kinetics at lithium/polymer interfaces. J. Electrochem. Soc. 152, A396. https://doi.org/10.1149/1.1850854.

12. Kazyak, E., Garcia-Mendez, R., LePage, W.S., Sharafi, A., Davis, A.L., Sanchez, A.J., Chen, K.-H., Haslam, C., Sakamoto, J., and Dasgupta, N.P. (2020). Li penetration in ceramic solid electrolytes: operando microscopy analysis of morphology, propagation, and reversibility. Matter 2, 1025–1048. https://doi.org/10.1016/j.matt.2020.02.008.

13. Porz, L., Swamy, T., Sheldon, B.W., Rettenwander, D., Frömling, T., Thaman, H.L., Berendts, S., Uecker, R., Carter, W.C., and Chiang, Y.-M. (2017). Mechanism of lithium metal penetration through inorganic solid

electrolytes. Adv. Energy Mater. 7, 1701003. https://doi.org/10.1002/aenm.201701003.

14. Zhao, F., Liang, J., Yu, C., Sun, Q., Li, X., Adair, K., Wang, C., Zhao, Y., Zhang, S., Li, W., et al. (2020). A versatile Sn-substituted argyrodite sulfide electrolyte for all-solid-state Li metal batteries. Adv. Energy Mater. 10, 1903422. https://doi.org/10.1002/aenm.201903422.

15. Gao, Y., Wang, D., Li, Y.C., Yu, Z., Mallouk, T.E., and Wang, D. (2018). Salt-based organic–inorganic nanocomposites: towards a stable lithium metal/Li10GeP2S12 solid electrolyte interface. Angew. Chem. Int. Ed. Engl. 57, 13608–13612. https://doi.org/10.1002/anie.201807304.

16. Shen, K., Wang, Z., Bi, X., Ying, Y., Zhang, D., Jin, C., Hou, G., Cao, H., Wu, L., Zheng, G., et al. (2019). Magnetic field–suppressed lithium dendrite growth for stable lithium-metal batteries. Adv. Energy Mater. 9, 1900260. https://doi.org/10.1002/aenm.201900260.

17. Chen, Y., Dou, X., Wang, K., and Han, Y. (2019). Lithium dendrites inhibition via diffusion enhancement. Adv. Energy Mater. 9, 1900019. https://doi.org/10.1002/aenm.201900019.

18. Ma, C., Rangasamy, E., Liang, C., Sakamoto, J., More, K.L., and Chi, M. (2015). Excellent stability of a lithium-ion-conducting solid electrolyte upon reversible Li+/H+ exchange in aqueous solutions. Angew. Chem. 127, 131–135. https://doi.org/10.1002/ange.201408124.

19. Fang, C., Lu, B., Pawar, G., Zhang, M., Cheng, D., Chen, S., Ceja, M., Doux, J.-M., Musrock, H., Cai, M., et al. (2021). Pressure-tailored lithium deposition and dissolution in lithium metal batteries. Nat. Energy 6, 987–994. https://doi.org/10.1038/s41560-021-00917-3.

20. Krauskopf, T., Dippel, R., Hartmann, H., Peppler, K., Mogwitz, B., Richter, F.H., Zeier, W.G., and Janek, J. (2019). Lithium-metal growth kinetics on LLZO garnet-type solid electrolytes. Joule 3, 2030–2049. https://doi.org/10.1016/j.joule.2019.06.013.

21. Krauskopf, T., Richter, F.H., Zeier, W.G., and Janek, J. (2020). Physicochemical concepts of the lithium metal anode in solid-state batteries. Chem. Rev. 120, 7745–7794. https://doi.org/10.1021/acs.chemrev.0c00431.

22. Doux, J.M., Nguyen, H., Tan, D.H.S., Banerjee, A., Wang, X., Wu, E.A., Jo, C., Yang, H., and Meng, Y.S. (2020). Stack pressure considerations for room-temperature all-solid-state lithium metal batteries. Adv. Energy Mater. 10, 1903253.

23. Chen, Y., Li, W., Sun, C., Jin, J., Wang, Q., Chen, X., Zha, W., and Wen, Z. (2021). Sustained release-driven formation of ultrastable SEI between Li6PS5Cl and lithium anode for sulfide-based solid-state batteries. Adv. Energy Mater. 11, 2002545. https://doi.org/10.1002/aenm.202002545.

24. Fan, X., Ji, X., Han, F., Yue, J., Chen, J., Chen, L., Deng, T., Jiang, J., and Wang, C. (2018). Fluorinated solid electrolyte interphase enables highly reversible solid-state Li metal battery. Sci. Adv. 4, eaau9245. https://doi.org/10.1126/sciadv.aau9245.

25. Zhang, Z., Chen, S., Yang, J., Wang, J., Yao, L., Yao, X., Cui, P., and Xu, X. (2018). Interface Re-

Engineering of Li10GeP2S12 Electrolyte and lithium anode for All-Solid-State lithium Batteries with Ultralong Cycle Life. ACS Appl. Mater. Interfaces 10, 2556–2565. https://doi.org/10.1021/acsami.7b16176.

26. Xu, H., Chien, P.-H., Shi, J., Li, Y., Wu, N., Liu, Y., Hu, Y.-Y., and Goodenough, J.B. (2019). High-performance all-solid-state batteries enabled by salt bonding to perovskite in poly(ethylene oxide). Proc. Natl. Acad. Sci. USA 116, 18815–18821. https://doi.org/10.1073/pnas.1907507116.

27. Li, Y., Wang, X., Zhou, H., Xing, X., Banerjee, A., Holoubek, J., Liu, H., Meng, Y.S., and Liu, P. (2020). Thin solid electrolyte layers enabled by nanoscopic polymer binding. ACS Energy Lett. 5, 955–961. https://doi.org/10.1021/acsenergylett.0c00040.

28. Xu, R., Han, F., Ji, X., Fan, X., Tu, J., and Wang, C. (2018). Interface engineering of sulfide electrolytes for all-solid-state lithium batteries. Nano Energy 53, 958–966. https://doi.org/10.1016/j.nanoen.2018.09.061.

29. Zhao, F., Alahakoon, S.H., Adair, K., Zhang, S., Xia, W., Li, W., Yu, C., Feng, R., Hu, Y., Liang, J., et al. (2021). An air-stable and Li-metal-compatible glass-ceramic electrolyte enabling high-performance all-solid-state Li metal batteries. Adv. Mater. 33, e2006577. https://doi.org/10.1002/adma.202006577.

30. Liang, J., Li, X., Zhao, Y., Goncharova, L.V., Li, W., Adair, K.R., Banis, M.N., Hu, Y., Sham, T.-K., Huang, H., et al. (2019). An Air-Stable and dendrite-free Li anode for highly stable all-solid-state sulfide-based Li batteries. Adv. Energy Mater. 9, 1902125. https://doi.org/10.1002/aenm.201902125.

31. Zheng, B., Zhu, J., Wang, H., Feng, M., Umeshbabu, E., Li, Y., Wu, Q.-H., and Yang, Y. (2018). Stabilizing Li10SnP2S12/Li interface via an in-situ formed solid electrolyte interphase layer. ACS Appl. Mater. Interfaces 10, 25473–25482. https://doi.org/10.1021/acsami.8b08860.

32. Xu, B., Li, X., Yang, C., Li, Y., Grundish, N.S., Chien, P.-H., Dong, K., Manke, I., Fang, R., Wu, N., et al. (2021). Interfacial chemistry enables stable cycling of all-solid-state Li metal batteries at high current densities. J. Am. Chem. Soc. 143, 6542–6550. https://doi.org/10.1021/jacs.1c00752.

33. Ye, L., and Li, X. (2021). A dynamic stability design strategy for lithium metal solid state batteries. Nature 593, 218–222. https://doi.org/10.1038/s41586-021-03486-3.

34. Tang, W., Tang, S., Zhang, C., Ma, Q., Xiang, Q., Yang, Y.-W., and Luo, J. (2018). Simultaneously enhancing the thermal stability, mechanical modulus, and electrochemical performance of solid polymer electrolytes by incorporating 2D sheets. Adv. Energy Mater. 8, 1800866. https://doi.org/10.1002/aenm.201800866.

35. Winter, M., and Brodd, R.J. (2004). What are batteries, fuel cells, and supercapacitors? Chem. Rev. 104, 4245–4269. https://doi.org/10.1021/cr020730k.

36. Zhao, F., Sun, Q., Yu, C., Zhang, S., Adair, K., Wang, S., Liu, Y., Zhao, Y., Liang, J., Wang, C., et al. (2020). Ultrastable anode interface

achieved by fluorinating electrolytes for all-solid-state Li metal batteries. ACS Energy Lett. *5*, 1035–1043. https://doi.org/10.1021/acsenergylett.0c00207.

37. Zhong, Y., Xie, Y., Hwang, S., Wang, Q., Cha, J.J., Su, D., and Wang, H. (2020). A highly efficient all-solid-state lithium/electrolyte interface induced by an energetic reaction. Angew. Chem. Int. Ed. Engl. 59, 14003–14008. https://doi.org/10.1002/anie.202004477.

38. Ji, X., Hou, S., Wang, P., He, X., Piao, N., Chen, J., Fan, X., and Wang, C. (2020). Solid-state electrolyte design for lithium dendrite suppression. Adv. Mater. *32*, e2002741. https://doi.org/10.1002/adma.202002741.

39. Han, F., Westover, A.S., Yue, J., Fan, X., Wang, F., Chi, M., Leonard, D.N., Dudney, N.J., Wang, H., and Wang, C. (2019). High electronic conductivity as the origin of lithium dendrite formation within solid electrolytes. Nat. Energy *4*, 187–196. https://doi.org/10.1038/s41560-018-0312-z.

40. Liu, X., Garcia-Mendez, R., Lupini, A.R., Cheng, Y., Hood, Z.D., Han, F., Sharafi, A., Idrobo, J.C., Dudney, N.J., Wang, C., et al. (2021). Local electronic structure variation resulting in Li 'filament' formation within solid electrolytes. Nat. Mater. *20*, 1485–1490. https://doi.org/10.1038/s41563-021-01019-x.

41. Lin, Y., Li, J., Lai, Y., Yuan, C., Cheng, Y., and Liu, J. (2013). A wider temperature range polymer electrolyte for all-solid-state lithium ion batteries. RSC Adv *3*, 10722–10730. https://doi.org/10.1039/C3RA40306H.

42. Zhang, X., Zhang, Q., Wang, X.G., Wang, C., Chen, Y.N., Xie, Z., and Zhou, Z. (2018). An extremely simple method for protecting lithium anodes in Li-O2 batteries. Angew. Chem. Int. Ed. Engl. *57*, 12814–12818.

43. Liang, J., Li, X., Wang, S., Adair, K.R., Li, W., Zhao, Y., Wang, C., Hu, Y., Zhang, L., Zhao, S., et al. (2020). Site-occupation-tuned superionic LixScCl3+ x halide solid electrolytes for all-solid-state batteries. J. Am. Chem. Soc. *142*, 7012–7022. https://doi.org/10.1021/jacs.0c00134.

44. Shi, X., Zeng, Z., Sun, M., Huang, B., Zhang, H., Luo, W., Huang, Y., Du, Y., and Yan, C. (2021). Fast Li-ion conductor of Li3HoBr6 for stable all-solid-state lithium–sulfur battery. Nano Lett. *21*, 9325–9331. https://doi.org/10.1021/acs.nanolett.1c03573.

45. Wenzel, S., Randau, S., Leichtweiß, T., Weber, D.A., Sann, J., Zeier, W.G., and Janek, J. (2016). Direct observation of the interfacial instability of the fast ionic conductor Li10GeP2S12 at the lithium metal anode. Chem. Mater. *28*, 2400–2407. https://doi.org/10.1021/acs.chemmater.6b00610.

46. Wang, C., Liang, J., Luo, J., Liu, J., Li, X., Zhao, F., Li, R., Huang, H., Zhao, S., Zhang, L., et al. (2021). A universal wet-chemistry synthesis of solid-state halide electrolytes for all-solid-state lithium-metal batteries. Sci. Adv. *7*, eabh1896. https://doi.org/10.1126/sciadv.abh1896.

47. Wenzel, S., Sedlmaier, S.J., Dietrich, C., Zeier, W.G., and Janek, J. (2018). Interfacial reactivity and interphase growth of argyrodite solid electrolytes at lithium metal electrodes. Solid State Ion *318*, 102–112.

48. Wang, C., and Hong, J. (2007). Ionic/electronic conducting characteristics of LiFePO4 cathode materials. Electrochem. Solid State Lett. *10*, A65. https://doi.org/10.1149/1.2409768.

49. Ma, L., Schroeder, M.A., Borodin, O., Pollard, T.P., Ding, M.S., Wang, C., and Xu, K. (2020). Realizing high zinc reversibility in rechargeable batteries. Nat. Energy *5*, 743–749. https://doi.org/10.1038/s41560-020-0674-x.

50. Zheng, J., Zhao, Q., Tang, T., Yin, J., Quilty, C.D., Renderos, G.D., Liu, X., Deng, Y., Wang, L., Bock, D.C., et al. (2019). Reversible epitaxial electrodeposition of metals in battery anodes. Science *366*, 645–648. https://doi.org/10.1126/science.aax6873.

51. Li, Q., Chen, A., Wang, D., Pei, Z., and Zhi, C. (2022). "Soft Shorts" hidden in zinc metal anode research. Joule *6*, 273–279. https://doi.org/10.1016/j.joule.2021.12.009.

52. Homann, G., Stolz, L., Nair, J., Laskovic, I.C., Winter, M., and Kasnatscheew, J. (2020). Poly(ethylene oxide)-based electrolyte for solid-state-lithium-batteries with high voltage positive electrodes: evaluating the role of electrolyte oxidation in rapid cell failure. Sci. Rep. *10*, 4390. https://doi.org/10.1038/s41598-020-61373-9.

53. Sahore, R., Du, Z., Chen, X.C., Hawley, W.B., Westover, A.S., and Dudney, N.J. (2021). Practical considerations for testing polymer electrolytes for high-energy solid-state batteries. ACS Energy Lett. *6*, 2240–2247. https://doi.org/10.1021/acsenergylett.1c00810.

54. Sahore, R., Yang, G., Chen, X.C., Tsai, W.-Y., Li, J., Dudney, N.J., and Westover, A. (2022). A bilayer electrolyte design to enable high-areal-capacity composite cathodes in polymer electrolytes based solid-state lithium metal batteries. ACS Appl. Energy Mater. *5*, 1409–1413. https://doi.org/10.1021/acsaem.2c00050.

55. Liu, L., Xu, J., Wang, S., Wu, F., Li, H., and Chen, L. (2019). Practical evaluation of energy densities for sulfide solid-state batteries. eTransportation *1*, 100010. https://doi.org/10.1016/j.etran.2019.100010.

56. Wang, C., Liang, J., Zhao, Y., Zheng, M., Li, X., and Sun, X. (2021). All-solid-state lithium batteries enabled by sulfide electrolytes: from fundamental research to practical engineering design. Energy Environ. Sci. *14*, 2577–2619. https://doi.org/10.1039/D1EE00551K.

57. Balaish, M., Gonzalez-Rosillo, J.C., Kim, K.J., Zhu, Y., Hood, Z.D., and Rupp, J.L.M. (2021). Processing thin but robust electrolytes for solid-state batteries. Nat. Energy *6*, 227–239. https://doi.org/10.1038/s41560-020-00759-5.

58. Yang, X., Adair, K.R., Gao, X., and Sun, X. (2021). Recent advances and perspectives on thin electrolytes for high-energy-density solid-state lithium batteries. Energy Environ. Sci. *14*, 643–671. https://doi.org/10.1039/D0EE02714F.

59. Hippauf, F., Schumm, B., Doerfler, S., Althues, H., Fujiki, S., Shiratsuchi, T., Tsujimura, T., Aihara, Y., and Kaskel, S. (2019). Overcoming binder limitations of sheet-type solid-state cathodes using a solvent-free dry-film approach. Energy Storage Mater *21*, 390–398. https://doi.org/10.1016/j.ensm.2019.05.033.

60. Zhang, Z., Wu, L., Zhou, D., Weng, W., and Yao, X. (2021). Flexible sulfide electrolyte thin membrane with ultrahigh ionic conductivity for all-solid-state lithium batteries. Nano Lett. *21*, 5233–5239. https://doi.org/10.1021/acs.nanolett.1c01344.

61. Randau, S., Weber, D.A., Kötz, O., Koerver, R., Braun, P., Weber, A., Ivers-Tiffée, E., Adermann, T., Kulisch, J., Zeier, W.G., et al. (2020). Benchmarking the performance of all-solid-state lithium batteries. Nat. Energy *5*, 259–270. https://doi.org/10.1038/s41560-020-0565-1.

62. Wang, C., Yu, R., Duan, H., Lu, Q., Li, Q., Adair, K.R., Bao, D., Liu, Y., Yang, R., Wang, J., et al. (2022). Solvent-free approach for interweaving freestanding and ultrathin inorganic solid electrolyte membranes. ACS Energy Lett. *7*, 410–416. https://doi.org/10.1021/acsenergylett.1c02261.

63. Xiao, J., Li, Q., Bi, Y., Cai, M., Dunn, B., Glossmann, T., Liu, J., Osaka, T., Sugiura, R., Wu, B., et al. (2020). Understanding and applying coulombic efficiency in lithium metal batteries. Nat. Energy *5*, 561–568. https://doi.org/10.1038/s41560-020-0648-z.